



OPEN

Contribution of self- and other-regarding motives to (dis)honesty

Anastasia Shuster^{1,2}✉ & Dino J. Levy^{1,2}

Why would people tell the truth when there is an obvious gain in lying and no risk of being caught? Previous work suggests the involvement of two motives, self-interest and regard for others. However, it remains unknown if these motives are related or distinctly contribute to (dis)honesty, and what are the neural instantiations of these motives. Using a modified Message Game task, in which a Sender sends a dishonest (yet profitable) or honest (less profitable) message to a Receiver, we found that these two motives contributed to dishonesty independently. Furthermore, the two motives involve distinct brain networks: the LPFC tracked potential value to self, whereas the rTPJ tracked potential losses to other, and individual differences in motives modulated these neural responses. Finally, activity in the vmPFC represented a balance of the two motives unique to each participant. Taken together, our results suggest that (dis)honest decisions incorporate at least two separate cognitive and neural processes—valuation of potential profits to self and valuation of potential harm to others.

Why do people lie so often, even though honesty is a social norm? Then again, why would they tell the truth, in the face of possible monetary gain and no chance of punishment? Previous research suggests that the decision to lie or tell the truth depends on (1) the size of the profit to oneself gained from lying (self-interest), and (2) the degree of harm that the lie would cause to others (regard for others)¹. Other self-related motives, such as the chance of being caught², maintaining a positive self-image^{2,3}, and an aversion to lying⁴ also decrease dishonesty. Less research has looked into how *outcomes* of dishonest behaviour affect it¹. Indeed, lies are often self-serving but at the same time they are also other-harming (though not always^{5,6}). Moreover, the *degree* to which a given opportunity to lie is self-serving and other-harming varies from one scenario to the other. For example, the amount of money in a wallet found on the street entails both the potential profit for the finder and the loss for the owner. Recently, researchers found that the more money a wallet held, the *more* likely people were to surrender it to the police⁷. This supports the observation that people are sensitive to their own payoff as well as another's loss when confronted with a moral choice. However, it is not clear whether the two pieces of information distinctly affect behaviour, and whether people vary in the degree to which either self- or other-regarding motives drive their behaviour. The neural computation underlying the arbitration between these conflicting motives remains elusive as well.

When studying deception, researchers often use so-called instructed lying paradigms^{8,9}. Although they enable significant experimental control, they suffer from low ecological validity. In these tasks, participants do not benefit from lying (thus nullifying the conflict between moral values and self-interest). More importantly, lying in such scenarios has no social consequences, since the tasks are non-interactive and the lie does not harm anyone (thus nullifying the conflict between self-interest and regard for others' wellbeing⁹). Recently, a group of researchers put forward a signalling framework drawing from game theory¹⁰ to study spontaneous dishonesty⁸ in socially interactive settings¹¹, preserving the conflicts of real-life dishonesty. We used a modified version of one such task, the Message Game, in which a *Sender* sends either a truthful or a deceiving message to a *Receiver* regarding which of two options to choose. The task conflicts monetary gain to the Sender with honesty, to invoke internally-motivated lying. As potential profits to the Sender go up, Senders tend to send the deceptive message more often. Conversely, as potential losses to the Receivers rise, Senders lie less¹. By systematically varying the payoffs to both players, we can estimate the role of self- and other-regarding motives in dishonest choices and track their neural correlates. In the original Message Game, Sender's message does not always predict the Receiver's choice^{1,4}. This can lead to strategic choices, in which a Sender might choose to tell the truth while having the intention

¹Sagol School of Neuroscience, Tel Aviv University, Tel Aviv, Israel. ²Coller School of Management, Tel Aviv University, Tel Aviv, Israel. ✉email: Anastasia.Shuster@mssm.edu

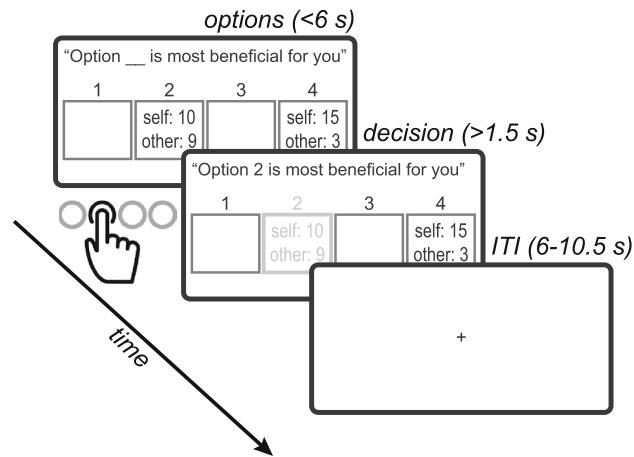


Figure 1. Trial timeline. On each trial, the participant (a “Sender”) chose which message to send to the Receiver, out of four options. The text at the top of the screen is the message that would be sent on this trial to the Receiver. Four options are revealed, each one consisting of some amount of money for the Sender (“self”) and some for the Receiver (“other”). One option was always truthful (the one more beneficial for the Receiver; #2 in the example) and one deceptive (#4). Payoffs to both players and locations varied between trials. The Sender had 6 s to indicate her choice, after which the chosen option was highlighted and stayed on the screen for the remainder of the trial.

to deceive¹². Therefore, we modified the task to include two options of \$0 to both players. Thus, deviating from the Sender’s message would result in a 66% chance of not winning money at all. This modification ensures that Senders’ choices have true consequences for their partners—a central component in our study.

Neuroimaging studies consistently implicate several regions of the prefrontal cortex (PFC) in generating dishonest behaviour^{11,13–18}. For example, deceptive responses—but not erroneous ones—selectively activate the middle frontal gyrus^{14,19}. Purposefully withholding information from the experimenter engages the anterior cingulate cortex, dorsolateral prefrontal cortex (dlPFC), and inferior and superior frontal gyrus^{20–23}. Because most studies employed paradigms with no interpersonal interaction¹¹ and thus no real consequences on another person, the neural correlates of the *social* aspect of deception are less well understood. However, there is plentiful evidence for the integration of other-regarding motives with self-interest during decision-making, coming from studies of prosocial behaviour. Even in the absence of explicit extrinsic pressure, humans are willing to forego monetary gain to cooperate²⁴, share resources^{25–27} and act fairly²⁸. Prosocial behaviour activates areas of the neural valuation system, consisting of the ventromedial prefrontal cortex (vmPFC) and ventral striatum^{26,28} (for reviews see^{29,30}). In these regions, social (e.g., norms) and non-social (e.g., monetary profit) factors are integrated into a common decision-value, which then gives rise to choice^{31–33}. Putatively, when choices present a conflict between one’s own profit and normative social principles, the valuation system interacts with areas typically involved in social cognition (e.g., the temporoparietal junction (TPJ)³⁴ or the posterior superior temporal sulcus (STS)²⁷) to compute the subjective value of an alternative³⁰. In the present study, we focus on the unique contribution of self- and other-regarding motives driving (dis)honest behaviour, as well as the combination of the two by the valuation system.

Participants played as Senders, choosing between honest and dishonest alternatives while inside the fMRI scanner. Choosing the dishonest option resulted in higher gains for themselves and greater losses to their partner compared to the honest alternative. Our first aim was to measure how increases to own profit and other’s loss affect dishonest choices. Our second aim was to explore individual differences in these motives. Third, we aimed to identify the neural activity associated with the two value parameters that drive dishonest behaviour—value to self and other. Finally, we examined how the neural representation of these value parameters reflects individual differences in behaviour.

Results

Behaviour. On each trial in the task, the participant (*Sender*) chose to send either a truthful or a deceptive message to the *Receiver* (see Fig. 1). We started with a simple measure of overall dishonesty—on how many of the trials did participants choose to send the deceptive message. The deceptive message was sent on almost half of the trials, but with substantial variability between participants ($45.45\% \pm 17.7\%$; range: 17.36–89.93%). Overall dishonesty did not differ statistically between female and male participants (females: $43\% \pm 15.9\%$ males: $50.59\% \pm 21\%$; $t(27) = -1.06$, $p = 0.29$, two-tailed two-sample t-test). Participants took on average 2.87 s to choose, and average reaction times for Truth choices (2.86 ± 0.45 s) did not differ from reaction times for Lie choices (2.88 ± 0.55 s; $t(27) = 0.4$, $p = 0.69$). The difference between honest and dishonest decision times, however, was significantly related to the individual differences in overall dishonesty: participants who lied more often took longer to tell the truth, whereas more honest participants took longer to lie ($r(26) = -0.8$, $p < 0.0001$; Fig. 2a). This suggests that the decision process reflects individual differences in dishonesty preference, not only in which alternative is chosen but also in the time it takes to choose.

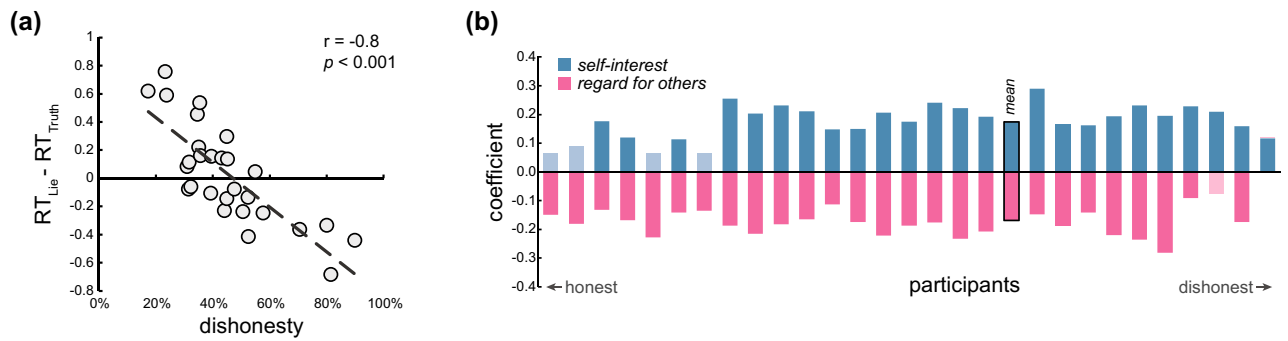


Figure 2. Behavioural results ($n = 28$). **(a)** Reaction times correlate with overall dishonesty. The average difference between Lie reaction times and Truth reaction times are on the y-axis, and percentage of dishonest trials on the x-axis. Each circle represents a subject. **(b)** Participants are arranged from most honest (far left) to most dishonest (far right). Bars represent each participant's regression coefficients, reflecting how much self-interest and regard for others contributed to their probability to lie. Greyed-out bars indicate non-significant coefficients.

Motives for (dis)honesty. To uncover what drove dishonest behaviour, we conducted a regression analysis of the probability to lie as a function of the potential payoffs, separately for each participant. The regression revealed that both the potential profits for the Sender (*value to self*; ΔV_{self}) and the potential losses to the Receiver (*value to other*; ΔV_{other}) affected the behaviour of most participants (Fig. 2b). This result was robust even after we added an interaction term ($\Delta V_{\text{self}} \times \Delta V_{\text{other}}$), door location, and time in the experiment to the model, or used a logistic regression instead of a linear one (see Supplementary Materials). A large ΔV_{self} coefficient implies a more *self-interested* participant: each unit of money to the Sender causes a bigger increase in the probability to lie, compared to a small ΔV_{self} coefficient. In other words, self-interest represents the sensitivity of a person to their own profit when faced with temptation. Note, that a high ΔV_{self} coefficient (more sensitive to own profit) does not imply that this person is necessarily more dishonest overall (which is given by the regression's intercept), but rather that when considering whether to lie or not, her own profit plays a more significant role in the decision. Similarly, a large ΔV_{other} coefficient (high *regard for others*) means that the loss to the Receiver greatly decreases the probability of the Sender to lie, compared to a small coefficient. While the average contribution of both parameters was similar in absolute terms ($\beta \Delta V_{\text{self}}$: 0.174 ± 0.06 , $\beta \Delta V_{\text{other}}$: $M = -0.169 \pm 0.057$, $t(27) = 0.35$, $p = 0.73$, paired two-tailed t-test), they varied substantially between participants ($\beta \Delta V_{\text{self}}$ range: 0.06 – 0.29 ; $\beta \Delta V_{\text{other}}$ range: -0.28 to 0.004). The fact that both coefficients were significant for the majority of participants implies that self-interest and regard for others distinctly affect the probability of the Sender to lie. This distinction is further strengthened by a lack of correlation between the two coefficients across participants ($r(26) = -0.2$, $p = 0.3$; Supplementary Figure S2).

Neuroimaging. Neural correlates of dishonesty. To identify neural correlates of dishonest behaviour, we contrasted the neural response during trials in which participants lied (i.e., sent the deceptive message) with trials in which they told the truth, controlling for reward amount. Consistent with previous studies of deception^{11,15}, we found several regions, including the medial PFC, left dlPFC, and bilateral insula. The opposite comparison (Truth > Lie) revealed activations in the right TPJ, right STS and cerebellum (see Table 1 and Supplementary Fig. S3).

Chosen value. To identify voxels responding to the Sender's reward magnitude in the chosen alternative vs. the unchosen one, we parametrically modelled the Sender's expected reward based on her choice and looked within the value system³⁵. Consistent with previous findings^{35,36}, the amount of money in the chosen vs. the unchosen option for the Sender positively correlated with the BOLD signal in the valuation system—the vmPFC and bilateral ventral striatum (see Fig. 3a).

Value to self and other. Value to Self. We found that the left lateral prefrontal cortex (LPFC) and intraparietal lobule, among other regions, negatively tracked the amount of money a Sender can gain from lying (ΔV_{self} ; Table 1, Fig. 3b). That is, a smaller potential profit from lying corresponded to a higher activation in the left LPFC and IPL. To examine how individual differences in self-interest affect this neural activity, we extracted the BOLD coefficients for ΔV_{self} from an independently defined region of interest (ROI) of the LPFC (MNI coordinates x, y, z : $-48, 6, 28$ ³⁷) and correlated them with $\beta \Delta V_{\text{self}}$ estimated using participants' behaviour. We found a positive significant neural-behaviour correlation ($r(25) = 0.42$, $p = 0.027$), where less self-interested participants show more deactivations of the LPFC.

Value to Other. To identify voxels tracking the value the Sender exerts toward the Receiver (i.e., value to other, ΔV_{other}), we regressed the potential monetary loss to the Receiver if the Sender chooses to act dishonestly ($\$Other_{\text{Lie}} - \$Other_{\text{Truth}}$). We found an inverse relationship between the activity of the rTPJ and Receiver's potential loss, such that higher potential losses to the Receiver deactivated the rTPJ (Table 1; Fig. 3c). We further extracted neural responses from the rTPJ using an independently-defined ROI (MNI coordinates x, y, z : $54, -58, 22$ ^{37,38}) and examined whether differences between participants in the activity of the rTPJ can be explained by individual

Contrast	Brain area	MNI coordinate			T	Cluster size
		x	y	z		
Truth vs. lie	Medial PFC	-3	29	38	4.06	128
	(Left) dorsolateral PFC	-47	31	28	3.93	23
	(Left) insula	-34	23	-2	4	31
	(Right) insula	30	25	-2	4.37	29
	(Right) TPJ	64	-28	-25	-4.02	116
	(Left) superior temporal sulcus	-58	-18	-5	-4.09	43
	Cerebellum	-9	-65	-5	-4.44	81
Value to self (ΔV_{self})	(Left) lateral PFC	-44	16	31	-3.53	409
	(Right) IPL	36	-50	47	-3.62	474
	(Left) IPL	-26	-54	39	-3.6	1,471
	Pre-SMA	-2	15	50	-3.42	51
	(Left) occipital	-45	-67	4	-3.33	72
	(Right) occipital	45	-77	-3	-3.4	168
	(Medial) occipital	-15	-70	1	-3.57	666
	Cerebellum	5	-64	-39	-3.35	63
	(Right) amygdala	28	-4	-14	-3.5	46
Value to other (ΔV_{other})	(Right) TPJ	45	-52	24	-3.37	33
	Precuneus	-7	-63	44	3.79	21
	(Left) thalamus	-6	-18	11	3.37	26
	Cuneus	-6	-92	22	3.36	32
	(Left) occipital	-9	-73	3	-3.4	115
	(Right) occipital	9	-73	-8	-3.42	108

Table 1. List of whole-brain contrast results. *PFC* prefrontal cortex, *IPL* inferior parietal cortex, *TPJ* temporoparietal junction, *SMA* supplementary motor area.

differences in their other-regarding motive for lying. We found that participants with low regard for others showed rTPJ deactivation, whereas in those who have high regard for others, higher potential losses elicit *more* activity in the rTPJ ($r(25) = 0.51, p = 0.006$). That is, the degree to which social consequences affect an individual's behaviour is related to how these social consequences are represented in the rTPJ.

Balanced self-other representation. To understand how the vmPFC tracks competing values and motives, we looked for differences between neural sensitivity to value to self and value to other in the valuation system, and how self- and other-regarding motives affect this activity. To do so, we first computed for each participant an *other-self differential* score ($\beta\Delta V_{\text{other}} - \beta\Delta V_{\text{self}}$), indicating how much a participant's behaviour is driven by one motive or the other. High positive scores indicate a higher contribution of other-regarding motives, whereas high negative scores suggest more contribution of self-regarding motives. Then, we compared the neural activity tracking value to other with that of value to self ($\Delta V_{\text{other}} > \Delta V_{\text{self}}$) in the valuation system. This contrast yielded an empty map. However, when we regressed onto this map each participant's *other-self differential* score, we identified a cluster of voxels located in the vmPFC (MNI coordinate x, y, z: 9, 41, -8; Fig. 4). The vmPFC was more active for ΔV_{self} compared to ΔV_{other} in self-interested participants. Conversely, for other-regarding participants, who place higher weight on ΔV_{other} compared to ΔV_{self} , the vmPFC was more active for ΔV_{other} compared to ΔV_{self} ($r(25) = 0.49, p = 0.009$). Thus, the vmPFC represents in each participant her own *idiosyncratic balance* between value to self and value to other. This finding is consistent with the role of the vmPFC as an integrator of various attributes of choice to one single value.

Discussion

Using a modified Message task, we found that both self-interest and regard for others contribute independently to (dis)honesty. Crucially, our results suggest that these motives rely on distinct neural processes, with self-interest involving the lateral prefrontal and parietal cortices, and regard for others the right temporoparietal junction, among others. Furthermore, we find a combination of motives in the vmPFC, consistent with its known role as an integrator of value. That is, in self-interested participants, the vmPFC was more sensitive to one's own payoffs than losses to another; conversely, in other-regarding participants, the vmPFC showed higher activity for their partner's potential losses than to their own potential gains.

Previous research has indicated that increasing the consequences of the lie decreases its occurrence¹. We have extended this notion to elucidate individual differences in this sensitivity, and thanks to our within-participant design and orthogonality of the regressors, we captured independent self- and other-regarding motives. The significant effect of both motives means they explain *distinct* portions of the variance in behaviour, suggesting they are separate processes. This notion is further supported by the distinct neural networks associated with each

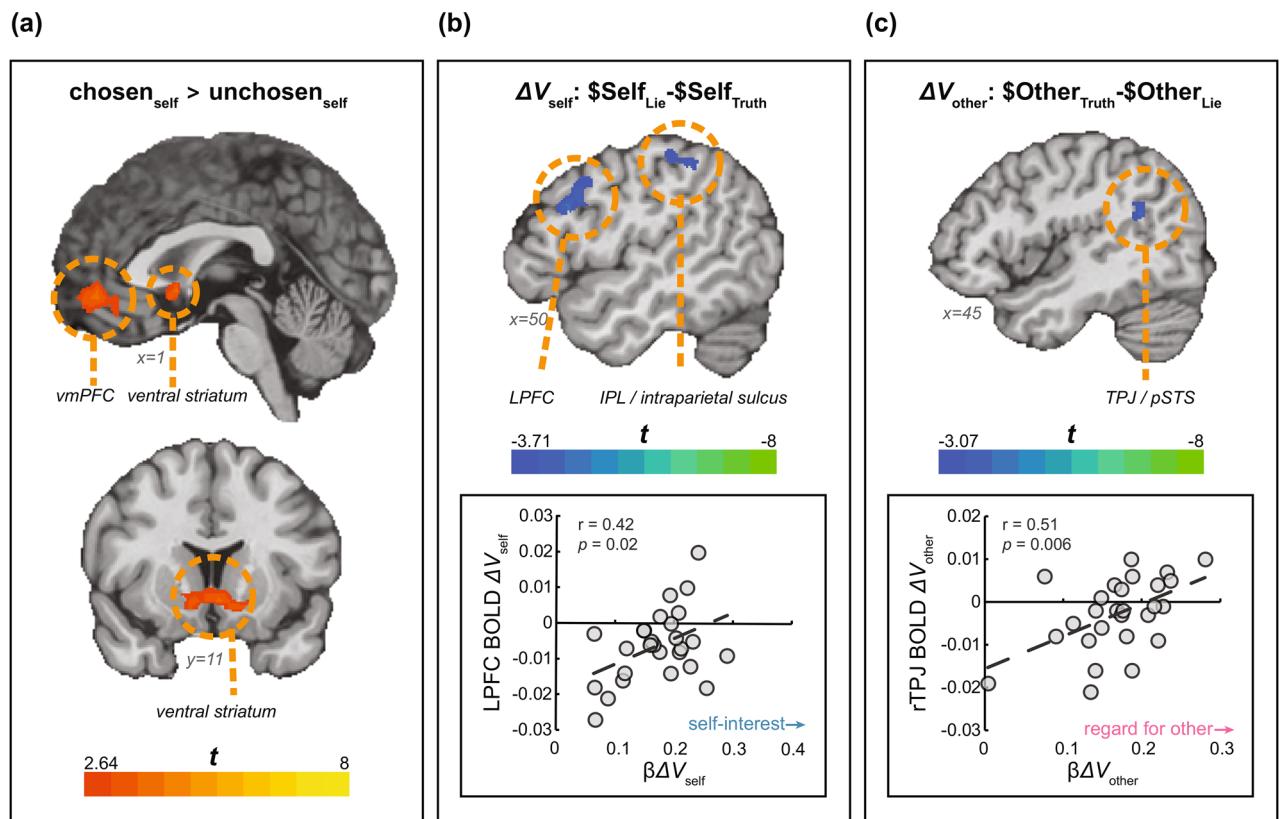


Figure 3. Neural sensitivity to values ($n=27$). (a) Amount of money for the Sender in the chosen option vs. the unchosen option. The activation map was masked using value-related ROIs taken from a meta-analysis (Bartra et al., 2013). Map at $q(\text{FDR})=0.05$. (b) Voxels sensitive to Sender's potential profits from dishonesty (value for self; ΔV_{self}) (top). For visualization purposes, the map is thresholded at $p=0.001$, cluster-size corrected. The BOLD response in the LPFC is positively correlated with the behavioural measure of self-interest (bottom). (c) Voxels sensitive to Receiver's potential losses from dishonesty (value for other; ΔV_{other}) (top). Map thresholded at $p=0.005$, cluster-size corrected. The BOLD response in the rTPJ is positively correlated with the behavioural measure of regard for others.

motive. Furthermore, the insignificant effect of the interaction term for most participants suggests that for the most part, they are also *independent* from each other, that is, that the influence of value to self is similar across different levels of value to other, and vice versa.

This distinction coincides with the observation that some people would not lie, even if lying would *help* another person (as in a case of a white lie³⁹), suggesting that for some people, the self-regarding motive is the *only* motive driving behaviour and that honesty can be wholly unrelated to the consequence of lying. Furthermore, Bizou-van-Pol and colleagues (2015)⁴⁰ demonstrated that a prosocial tendency—measured using the Dictator game and the Prisoner's Dilemma Game—is differentially linked to self-benefitting lying and other-benefitting lying. While the willingness to lie for the benefit of others is positively linked to prosociality, lying for one's own benefit is negatively linked to it. Taken together, these findings strengthen the conclusion that lying consists of at least two distinct components guiding decision-making—own and other's outcomes.

Some previous studies reported that time pressure and cognitive load increase dishonesty⁴¹, suggesting that honesty is the more natural and automatic response, whereas acting dishonestly requires deliberation. Our evidence does not line up with this interpretation of the data. In general, in the context of choices, differences in reaction times should be interpreted carefully. Reaction times could attest to the ease of choice^{42,43}, or to the rate in which evidence accumulates in favour of one of the alternatives⁴⁴, which is related to the strength-of-preferences⁴³. Although all participants were faced with the same choice set, variation in their preferences yielded variations in decision times. Along the same lines as previous findings⁴³, we find that honest participants are quicker to tell the truth, whereas dishonest participants are quicker to lie. In other words, acting out of character takes longer. This result goes against dual-process models, which assume similar preferences for all participants (e.g., everyone is honest at heart, and lying requires extra time to overcome the honesty urge).

We find that potential profits from lying involve the LPFC, dovetailing some recent research elucidating its role in moral decision-making⁴⁵. Lesions to the dlPFC were found to reduce honesty concerns in favour of self-interest⁴⁶, suggesting it is causally involved in arbitrating the two. Further evidence comes from a stimulation study⁴⁷, in which activating the dlPFC increased honesty. Interestingly, this was only true when a conflict existed between self-interest and honesty, suggesting that, as the authors describe it, the role of the dlPFC is to represent the psychological cost of being dishonest. The LPFC was also implicated in another type of moral

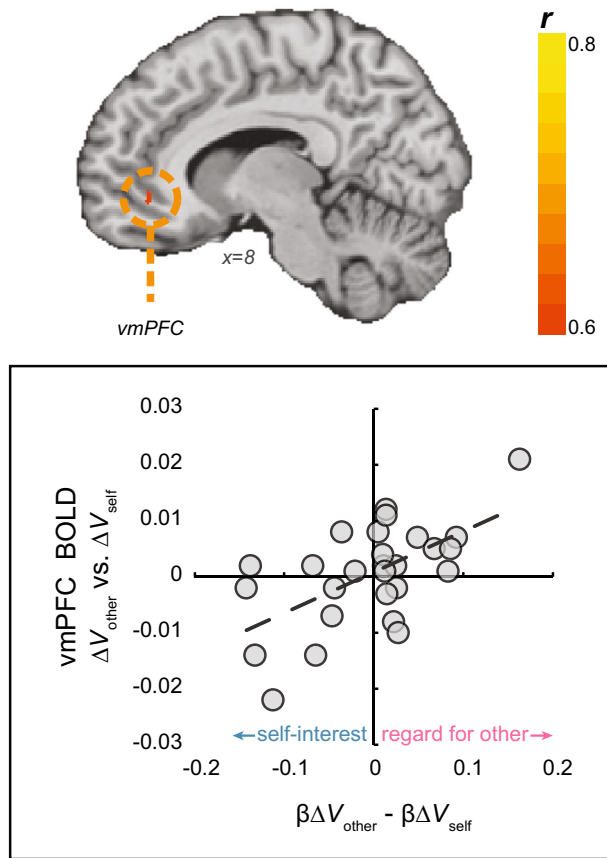


Figure 4. Value to self vs. value to other, modulated by preferences ($N = 27$). Contrasting potential profit for Sender (value to self; ΔV_{self}) with potential losses to Receiver (value to other; ΔV_{other}), modulated by individual differences in the balance between regard for other and self-interest. The activation map was masked using value-related ROIs taken from a meta-analysis (Bartra et al., 2013).

decision-making, when the harm to another individual is physical (electric shocks) rather than monetary³⁷. Not only did the LPFC negatively represent potential ill-gotten gains, but individual differences in harm-aversion correlated with the activity in the LPFC. Specifically, activity in this region decreased as the amount of money that could be gained grew, paralleling our own findings in a different task and another moral domain. The authors attributed this finding to a sense of blame, showing that the LPFC encodes the level of blameworthiness—higher gains are associated with lower blame and hence lower activity in the LPFC, echoing the notion of psychological cost. Taken together, these studies, along with our own, support the role of the LPFC as a context-specific modulator of decision-relevant information⁴⁵.

As for the other-regarding motive to act honestly, we find that the right TPJ negatively tracks the value for other (ΔV_{other}). We further find that the rTPJ encodes the Receiver's loss positively in participants who care more about it. Thus, the sensitivity of the rTPJ to consequences of dishonesty can drive some individuals to act prosocially and others selfishly. Interestingly, although this area has been implicated in deception, it does not show up in the overlap between deception-related and executive-control-related brain maps¹⁵, suggesting that it may represent a different aspect of dishonesty. We propose that this aspect is its social consequences. Our hypothesis is supported by a meta-analysis of deception studies, showing that the TPJ is specifically involved in interactive deception tasks¹¹, that is, only when a lie has implications on another participant. Indeed, the TPJ is a known hub in the social cognition neural network, selectively activated when interacting with social agents⁴⁸, and is thought to represent others' minds^{49–51}. The locus of our activation corresponds to the posterior rTPJ, an area highly connected with the vmPFC and implicated in a wide array of mentalizing tasks⁵¹. In the moral domain, the rTPJ is involved in forming judgments about others' moral acts^{52,53}. Here, we provide evidence that the potential outcomes of moral acts also involve the rTPJ. Moreover, we show that the individual's neural sensitivity to these potential outcomes can explain their social behaviour.

Finally, we find that the vmPFC represents a balance between competing values. Importantly, this balance in the vmPFC emerges only when accounting for the weight that each individual placed on their own and another's payoff, implying that the nature of this representation is subjective—personal preferences modulate the objective amounts of money. We find that if someone cares more about themselves than others, her valuation system will be more sensitive to her own profits. Alternatively, the valuation system of someone who is concerned with others more than with herself, would be more sensitive to others' profits. This balanced representation of value suggests a neural instantiation of observed differences in behaviour. Our findings are in line with abundant research on

the role of the vmPFC in value computation and representation^{27,32,33,46,54}, suggesting that when two values or motives conflict, the vmPFC represents a comparison of them.

There are at least two limitations to our study, both stemming from its design. First, we cannot fully disentangle self- and other-related motives from preferences for efficiency (maximizing both players' payoff) or equality (minimizing the difference between players' payoffs). This is due to the structure of the payoffs, in which the Lie option is usually more efficient and the Truth option is more equal. However, when we tested the effects of efficiency and equality on choice we found that value-to-self and value-to-other still have a role over and above the effect of efficiency and inequality (see Supplementary Materials for details). Nevertheless, future research should re-examine the effects demonstrated in the current study with a set of payoffs that are perfectly orthogonal in respect to efficiency and inequality. Second, because we did not assess participants' altruism levels, it is an open question whether our findings are specific to (dis)honest decision-making, or constitute a general prosocial phenomenon. Previous studies have looked into this, having the same participants complete both a Dictator Game and a Message Game^{1,46}, and found that honesty concerns operate above and beyond simple altruism. Furthermore, altruism is negatively associated with a self-related motive for lying and positively associated with an other-related motive for lying⁴⁰, suggesting a common neural and behavioural basis. Since other forms of social decision-making reveal neural patterns of activity consistent with our own^{37,55}, we hypothesize that our findings would generalize to altruism as well.

In summary, we found that internally-motivated dishonest behaviour⁹ varies dramatically between individuals, both in which motive drives behaviour and to what extent. Moreover, we find that two distinct motives can be identified from behaviour and traced back to separate neural activation patterns. At the behavioural level, individual's levels of self-interest and regard for others contribute independently to a choice to lie. On the neural level, the LPFC and rTPJ track value to self and value to other, respectively. Importantly, self- and other-regarding motives for (dis)honesty affect this sensitivity to value—in the LPFC, the rTPJ, and the valuation system. These findings suggest a neural instantiation of individual differences in behaviour; while prosocial individuals' neural valuation systems are more sensitive to others' wellbeing, those of selfish individuals are more sensitive to their own.

Materials and methods

Participants. Thirty-three participants enrolled in the study (22 females; age $M = 25.35$, 19–30). Participants gave informed written consent before participating in the study. All experimental protocols were approved by the Institutional Review Board at Tel-Aviv University, and all methods were carried out in accordance with the approved guidelines. All participants were right-handed, and had a normal or corrected-to-normal vision. Of the 33 participants, five were excluded from all analyses due to a lack of variability in their behavioural responses—they either lied on more than 90% ($n = 3$) or on less than 10% ($n = 2$) of the trials. Although arbitrary, this cut-off point was selected to ensure successful modelling of behaviour. An additional participant was excluded only from neural analyses due to excessive head movements during the scans (> 3 mm). Participants were paid a participation fee and the amount of money they won on a randomly drawn and implemented trial.

Experiment. Task. On each trial, the participant in the fMRI scanner (*Sender*) was asked to send the following message to her partner (*Receiver*): “Option ___ is most profitable for you”. Senders watched a screen with 4 ‘doors’. Two doors were empty (indicating payoffs of \$0 for both participants), and two doors contained non-zero payoff information for themselves and for their partner (the Receiver; see Fig. 1). Participants were given 6 s to indicate their choice by pressing one of four buttons on a response box. After choosing, the chosen door was highlighted and the message text changed accordingly (e.g., “Option 3 is most profitable for you”, if door 3 was chosen). The duration of this decision screen was set to have a minimum of 1.5 s and to make up for a total trial duration of 7.5 s. For example, if a participant made a choice after 3.5 s, the decision screen appeared for 4 s. If no choice was made in the allotted time, a “no choice” feedback screen appeared for 1.5 s. Afterwards, a fixation screen appeared for 6–10.5 s. Senders were told that the Receiver would view the message and choose which door to open, when the only available information for them is the door number, and the fact that two of the doors are empty. Both players' payoffs depended on the door the Receiver opened. To avoid reputation concerns, even after choice, the Receiver did not know how much the Sender got, nor what amounts of money were hidden behind the non-chosen doors.

Payoff structure. The payoffs were intended to create a conflict between honesty and monetary profit. On each trial, each door contained some amount of money for the Sender and some amount of money for the Receiver. A truthful message (*Truth* option) is defined as when the Sender is choosing the door (the message to send) that results in a larger amount of money for the Receiver. A deceptive message (*Lie* option) is defined as when the Sender is choosing the door that results in a smaller amount of money for the Receiver (and a larger amount of money for the Sender) compared to the Truth option. Payoffs varied on a trial-by-trial basis, ranging between 10–42₪ (1₪ \approx 0.3USD) for the Sender, and 1–31₪ for the Receiver (see Supplementary Table S1 and Supplementary Fig. S1 for a full list). Critically, the potential profits for the Sender from lying ($\Delta V_{\text{self}} = \$\text{Self}_{\text{Lie}} - \$\text{Self}_{\text{Truth}}$; range 0–12₪) varied independently from the potential losses for the Receiver ($\Delta V_{\text{other}} = \$\text{Other}_{\text{Truth}} - \$\text{Other}_{\text{Lie}}$; range 1–20₪; $r(38) = 0.25$, $p = 0.11$). Figure 1 depicts an example trial, in which choosing to tell the truth would result in 10₪ for the Sender and 9₪ for the Receiver, whereas lying would result in 15₪ for the Sender and only 3₪ for the Receiver. Hence, the Sender's potential profit (ΔV_{self}) is 5₪ (15 – 10), and the Receiver's potential loss (ΔV_{other}) is 6₪ (9 – 3). Importantly, to avoid any interfering motives (e.g. envy), all trials of interest (38 out of 40) had a higher payoff for the Sender than for the Receiver (the Sender was always better off than the Receiver, irrespective of the chosen door). Two *catch trials* offered a 0₪ payoff for the Sender from lying (i.e.,

$\$Self_{Lie} = \$Self_{Truth}$), with no conflict between honesty and gain for the Sender. These trials served to ensure the participants are attentive.

A key component of the task is the addition of two empty doors to each trial, containing zero money for each player (doors 1 & 3 in the Fig. 1 example). These options ensured that the message the Sender sends is indeed followed by the Receiver, because deviating from the recommended door may result in opening an empty door. Consider the example in Fig. 1: if the Sender chooses to lie, she sends a message regarding door #4. All the Receiver will see is that door #4 is highlighted. The Receiver does not know how much money is behind which door, but she does know that two of the doors have no money at all. Even if the Receiver believes she is lied to, it is in her best interest to open door #4, otherwise she (and the Sender) face a 66% chance of winning no money at all.

Procedure. Participants arrived to the Imaging Center and met the experimenter and a confederate acting as the Receiver. The confederate was always a Caucasian female, aged ~25. Both the Sender and Receiver read written instructions, signed consent forms and underwent a training stage of the task—playing as both the Sender and the Receiver. Training as Sender was intended to familiarize the participant with the Message Task. Training on the Receiver's role allowed them to experience what happens when the Receiver does not follow the recommended Message, and ensure they understood the consequences of sending a truthful or deceptive message.

Each participant completed four scans. Forty unique payoff trials were randomly interspersed in a given scan, making up 160 trials per participant (40 unique payoffs \times 4 repetitions). At the end of the experiment, one trial was selected randomly and presented to the Sender as the message that will be sent to the Receiver. In pilot studies in our lab, using real participants acting as Receivers, 100% chose according to the message sent by the Sender. Therefore, in the current study, we automatically set the Receiver's choice to be according to the Sender's message, and paid the Sender whichever amount was associated with that option.

After the scan, participants completed a short debriefing questionnaire. Debriefing consisted of several demographic questions and questions regarding the choices the participant made in the task. Specifically, we aimed to ensure participants were not suspicious of the confederate, by asking how the identity of the Receiver affected their choices.

Image acquisition and processing. Scanning was performed at the Strauss Neuroimaging Center at Tel Aviv University, using a 3 T Siemens Prisma scanner with a 64-channel Siemens head coil. Anatomical images were acquired using MPRAGE, which comprised 208 1-mm thick axial slices at an orientation of -30° to the AC-PC plane. To measure blood oxygen level-dependent (BOLD) changes in brain activity task performance, a T2*-weighted functional multi-band EPI pulse sequence was used (TR = 1.5 s; TE = 30 ms; flip angle = 70° ; matrix = 86×86 ; field of view (FOV) = 215 mm; slice thickness = 2.5 mm). 50 axial (-30° tilt) slices with no interslice gap were acquired in ascending interleaved order.

Brain Voyager QX (Brain Innovation) was used for image analysis, with additional analyses performed in Matlab. Functional images were sinc-interpolated in time to adjust for staggered slice acquisition, corrected for any head movement by realigning all volumes to the first volume of the scanning session using six-parameter rigid body transformations, and de-trended and high-pass filtered to remove low-frequency drift in the fMRI signal. Data were then spatially smoothed with a Gaussian kernel of 5 mm (full-width at half-maximum), co-registered with each participant's high-resolution anatomical scan and normalized using the Montreal Neurological Institute (MNI) template. All spatial transformations of the functional data used trilinear interpolation.

Behavioural analysis. *Overall deception & reaction times.* First, we removed no-response trials ($0.9\% \pm 1.2\%$ of trials), and trials in which participants chose an empty door (option of \$0 to both players; $1.4\% \pm 1.3\%$ of trials). Finally, we removed the catch trials (trials with identical payoffs to the Sender for Truth and Lie; $4.8\% \pm 0.03\%$ of trials). All further analyses were performed on this subset of trials ($92.7\% \pm 3.2\%$ of trials, range: 137–152 trials). We defined overall dishonesty rates per participant as the number of trials they lied out of this total number of trials.

Analysis of motives. To estimate the contribution of self- and other-regarding motives to dishonest behaviour, we fitted a linear regression per participant. Note, that there is increased variability in value-to-self compared to value-to-other. This was done for experimental reasons, to elicit sufficient lying. To allow us to still compare the regression coefficient across variables, we have z-transformed both variables. Then, for each unique payoff, we calculated each participant's probability to lie by averaging choices across the four repetitions, and that served as the dependent variable. The independent variables were normalized profits to self and losses to other (ΔV_{self} & ΔV_{other} respectively):

$$\text{probability}(\text{lie}) = \beta_0 + \beta_1 \widetilde{\Delta V}_{self} + \beta_2 \widetilde{\Delta V}_{other} + \varepsilon$$

where probability to lie ranges from 0 to 1, and \sim represents the z-transformed monetary amounts. We refer to the estimated coefficients as *self-interest* ($\beta \Delta V_{self}$) and *regard for others* ($\beta \Delta V_{other}$).

Statistical analyses. All reported t-tests are two-tailed. All reported correlations are Pearson correlations.

fMRI analysis. *Statistical significance.* For whole-brain analyses (*Neural correlates of dishonesty* and *Value to self and other* analyses), we used cluster-size threshold for multiple comparison correction. Cluster-defining threshold was set to 0.005, with 1,000 Monte Carlo simulations to achieve a family-wise error of 0.05.

For ROI analyses (*Chosen value*, *Motive Modulation of value to self and other*, and *Motive modulation of the value system*) we used an FDR < 0.05 threshold to correct for multiple comparisons.

Chosen value. To uncover voxels tracking the chosen value of each trial, we constructed a general linear model (GLM1) with the following predictors: (1) options period—a box-car function from trial onset until choice submission; (2) decision period—a box-car function from choice until ITI; and parametric modulators of the decision period: (3) chosen value—the amount of money (in €) that the Sender will receive in the chosen door; (4) unchosen value—the amount of money (in €) that the Sender would have received in the unchosen door; (5) Truth—an indicator function for trials in which the Sender told the truth; and (6) Lie—an indicator function for trials in which the Sender lied. All predictors were then convolved with HRF. Additional nuisance predictors included six motion-correction parameters and a mean signal from the ventricles, accounting for respiration. To reveal voxels tracking chosen value, we contrasted chosen value with unchosen value (predictors 3 and 4). We restricted the analysis to the valuation system only—the vmPFC and ventral striatum. We defined these areas using a mask generated from a meta-analysis of value studies³⁵ (consisting of 385 voxels).

Neural correlates of dishonesty. We used GLM1 to contrast Truth (trials in which the participant sent a truthful message) and Lie trials (in which the participant sent a deceptive message) in a whole-brain analysis. The “chosen value” predictor controlled for the amount of money participants stood to gain on each trial, to ensure that the observed patterns of neural response reflected (dis)honesty, irrespective of reward size.

Value for self and other. To identify neural correlates of value to self (ΔV_{self}) and value to other (ΔV_{other}), we constructed a second general linear model (GLM2) with the following predictors: (1) options period—a box-car function from trial onset to choice submission; (2) decision period—a box-car function from choice until ITI; and parametric modulators of the options period: (3) ΔV_{self} —the difference between the profit to Sender (in €) in the Lie option and the Truth option ($\$Self_{\text{Lie}} - \$Self_{\text{Truth}}$); (4) ΔV_{other} —the difference between profit to Receiver (in €) in the Truth option and the Lie option ($\$Other_{\text{Truth}} - \$Other_{\text{Lie}}$). All predictors were then convolved with HRF. Additional nuisance predictors included six motion-correction parameters and a mean signal from the ventricles, accounting for respiration.

Motive modulation of value to self and other. To inspect the regions sensitive to value (to self or other) for individual differences in motives, we conducted ROI analyses. For the value to self (ΔV_{self}) analysis, we focused on the LPFC and used an independently defined ROI³⁷, a sphere consisting of 25 voxels around MNI coordinates $-48, 6, 28$. We extracted the BOLD coefficients for ΔV_{self} (i.e., predictor 3 in GLM2) and correlated them with $\beta \Delta V_{\text{self}}$ estimated using participants’ behaviour. For the value to other (ΔV_{other}) analysis, we used a 25-voxel sphere centred on MNI coordinates $x, y, z: 54, -58, 22$, based on previous studies^{37,38}. We again extracted the BOLD signal, this time for ΔV_{other} (predictor 4 in GLM2) and correlated with behaviourally-estimated $\beta \Delta V_{\text{other}}$.

Motive modulation of the value system. To test how motives for dishonesty affect the valuation system, we started with computing for each participant an *other-self differential score* ($\beta \Delta V_{\text{other}} - \beta \Delta V_{\text{self}}$), indicating how much more one motive drives behaviour compared to the other. We then compared the neural activity tracking value to other with that of value to self ($\Delta V_{\text{other}} > \Delta V_{\text{self}}$) in the valuation system. We defined the valuation system using a mask generated from a meta-analysis of value studies³⁵ (consisting of 385 voxels). Finally, we regressed onto this map each participant’s other-self differential score, to identify motive-modulated value-representation. This analysis yielded a voxel-wise correlation map (correlating BOLD $\Delta V_{\text{other}} > \Delta V_{\text{self}}$ and behavioural $\beta \Delta V_{\text{other}} - \beta \Delta V_{\text{self}}$), as implemented in BrainVoyager.

Data availability

All statistical maps and computer code used to analyse the fMRI data are available on OSF.org (<https://osf.io/bvuxc/>).

Received: 30 December 2019; Accepted: 24 August 2020

Published online: 28 September 2020

References

- Gneezy, U. Deception: The role of consequences. *Am. Econ. Rev.* **95**, 384–394 (2005).
- Mazar, N., Amir, O. & Ariely, D. The dishonesty of honest people: A theory of self-concept maintenance. *J. Mark. Res.* **45**, 633–644 (2008).
- Jacobsen, C., Fosgaard, T. R. & Pascual-Ezama, D. Why do we lie? A practical guide to the dishonesty literature. *J. Econ. Surv.* **32**, 357–387 (2018).
- Gneezy, U., Rockenbach, B. & Serra-Garcia, M. Measuring lying aversion. *J. Econ. Behav. Organ.* **93**, 293–300 (2013).
- Pornpattananangkul, N., Zhen, S. & Yu, R. Common and distinct neural correlates of self-serving and prosocial dishonesty. *Hum. Brain. Mapp.* **39**, 3086–3103 (2018).
- Yin, L. & Weber, B. Can beneficial ends justify lying? Neural responses to the passive reception of lies and truth-telling with beneficial and harmful monetary outcomes. *Soc. Cogn. Affect Neurosci.* **11**, 423–432 (2016).
- Cohn, A., Maréchal, M. A., Tannenbaum, D. & Zünd, C. L. Civic honesty around the globe. *Science* **365**, 70–73 (2019).
- Yin, L., Reuter, M. & Weber, B. Let the man choose what to do: Neural correlates of spontaneous lying and truth-telling. *Brain Cogn.* **102**, 13–25 (2016).
- Sip, K. E., Roepstorff, A., McGregor, W. & Frith, C. D. Detecting deception: The scope and limits. *Trends Cogn. Sci.* **12**, 48–53 (2008).

10. Jenkins, A. C., Zhu, L. & Hsu, M. Cognitive neuroscience of honesty and deception: A signaling framework. *Curr. Opin. Behav. Sci.* **11**, 130–137 (2016).
11. Lisofsky, N., Kazzer, P., Heekeren, H. R. & Prehn, K. Investigating socio-cognitive processes in deception: A quantitative meta-analysis of neuroimaging studies. *Neuropsychologia* **61**, 113–122 (2014).
12. Volz, K. G., Vogeley, K., Tittgemeyer, M., von Cramon, D. Y. & Sutter, M. The neural basis of deception in strategic interactions. *Front. Behav. Neurosci.* **9**, 2 (2015).
13. Spence, S. A. *et al.* Behavioural and functional anatomical correlates of deception in humans. *NeuroReport* **12**, 2849–2853 (2001).
14. Abe, N. The neurobiology of deception: Evidence from neuroimaging and loss-of-function studies. *Curr. Opin. Neurol.* **22**, 594–600 (2009).
15. Christ, S. E., Essen, D. C. V., Watson, J. M., Brubaker, L. E. & Mcdermott, K. B. The contributions of prefrontal cortex and executive control to deception: Evidence from activation likelihood estimate meta-analyses. *Cereb Cortex* <https://doi.org/10.1093/cercor/bhn189> (2009).
16. Greene, J. D. & Paxton, J. M. Patterns of neural activity associated with honest and dishonest moral decisions. *Proc. Natl. Acad. Sci. USA* **106**, 12506–12511 (2009).
17. Sip, K. E. *et al.* The production and detection of deception in an interactive game. *Neuropsychologia* **48**, 3619–3626 (2010).
18. Abe, N. How the brain shapes deception: An integrated review of the literature. *Neuroscientist* **17**, 560–574 (2011).
19. Liang, C.-Y. *et al.* Neural correlates of feigned memory impairment are distinguishable from answering randomly and answering incorrectly: An fMRI and behavioral study. *Brain Cogn.* **79**, 70–77 (2012).
20. Kozel, A. F. *et al.* A pilot study of functional magnetic resonance imaging brain correlates of deception in healthy young men. *J. Neuropsychiatry* **16**, 295–305 (2004).
21. Kozel, F. A. *et al.* Detecting deception using functional magnetic resonance imaging. *Biol. Psychiatry* <https://doi.org/10.1016/j.biopsych.2005.07.040> (2005).
22. Langleben, D. D. *et al.* Telling truth from lie in individual subjects with fast event-related fMRI. *Hum. Brain Mapp.* **26**, 262–272 (2005).
23. Bhatt, S. *et al.* Lying about facial recognition: An fMRI study. *Brain Cogn.* **69**, 382–390 (2009).
24. Rilling, J. K. *et al.* A neural basis for social cooperation. *Neuron* **35**, 395–405 (2002).
25. Andreoni, J. & Miller, J. Giving according to GARP: An experimental test of the consistency of preferences for altruism. *Econometrica* **70**, 737–753 (2002).
26. Moll, J. *et al.* Human fronto-mesolimbic networks guide decisions about charitable donation. *Proc. Natl. Acad. Sci.* **103**, 15623–15628 (2006).
27. Hare, T. A., Camerer, C. F., Knoepfle, D. T. & Rangel, A. Value computations in ventral medial prefrontal cortex during charitable decision making incorporate input from regions involved in social cognition. *J. Neurosci.* **30**, 583–590 (2010).
28. Zaki, J. & Mitchell, J. P. Equitable decision making is associated with neural markers of intrinsic value. *Proc. Natl. Acad. Sci.* **108**, 19761–19766 (2011).
29. Fehr, E. & Camerer, C. F. Social neuroeconomics: the neural circuitry of social preferences. *Trends Cogn. Sci.* **11**, 419–427 (2007).
30. Ruff, C. C. & Fehr, E. The neurobiology of rewards and values in social decision making. *Nat. Rev. Neurosci.* **15**, 549–562 (2014).
31. Janowski, V., Camerer, C. & Rangel, A. Empathic choice involves vmPFC value signals that are modulated by social processing implemented in IPL. *Soc. Cogn. Affect. Neurosci.* **8**, 201–208 (2013).
32. Zaki, J., Lopez, G. & Mitchell, J. P. Activity in ventromedial prefrontal cortex co-varies with revealed social preferences: Evidence for person-invariant value. *Soc. Cogn. Affect. Neurosci.* **9**, 464–469 (2014).
33. Morelli, S. A., Sacchet, M. D. & Zaki, J. Common and distinct neural correlates of personal and vicarious reward: A quantitative meta-analysis. *NeuroImage* **112**, 244–253 (2015).
34. Smith, D. V., Clithero, J. A., Boltuck, S. E. & Huettel, S. A. Functional connectivity with ventromedial prefrontal cortex reflects subjective value for social rewards. *Soc. Cogn. Affect. Neurosci.* **9**, 2017–2025 (2013).
35. Bartra, O., McGuire, J. T. & Kable, J. W. The valuation system: A coordinate-based meta-analysis of BOLD fMRI experiments examining neural correlates of subjective value. *NeuroImage* **76**, 412–427 (2013).
36. Levy, D. J. & Glimcher, P. W. The root of all value: a neural common currency for choice. *Curr. Opin. Neurobiol.* <https://doi.org/10.1016/j.conb.2012.06.001> (2012).
37. Crockett, M. J., Siegel, J. Z., Kurth-Nelson, Z., Dayan, P. & Dolan, R. J. Moral transgressions corrupt neural representations of value. *Nat. Neurosci.* **20**, 879–885 (2017).
38. Bzdok, D. *et al.* Parsing the neural correlates of moral cognition: ALE meta-analysis on morality, theory of mind, and empathy. *Brain Struct. Funct.* **217**, 783–796 (2012).
39. Erat, S. & Gneezy, U. White lies. *Manage. Sci.* **58**, 723–733 (2012).
40. Bizziou-van-Pol, L., Haenen, J., Novaro, A., Occhipinti Liberman, A. & Capraro, V. Does telling white lies signal pro-social preferences? *Judg. Decis. Mak.* **10**, 538–548 (2015).
41. Capraro, V. The dual-process approach to human sociality: A review. arXiv:1906.09948 [physics, q-bio] (2019).
42. Milosavljevic, M., Malmaud, J., Huth, A., Koch, C. & Rangel, A. The drift diffusion model can account for the accuracy and reaction time of value-based choices under high and low time pressure. *SSRN Electron. J.* <https://doi.org/10.2139/ssrn.1901533> (2010).
43. Krajbich, I., Bartling, B., Hare, T. & Fehr, E. Rethinking fast and slow based on a critique of reaction-time reverse inference. *Nat. Commun.* **6**, 1–9 (2015).
44. Krajbich, I., Lu, D., Camerer, C. & Rangel, A. The attentional drift-diffusion model extends to simple purchasing decisions. *Front. Psychol.* **3**, 2 (2012).
45. Carlson, R. W. & Crockett, M. J. The lateral prefrontal cortex and moral goal pursuit. *Curr. Opin. Psychol.* **24**, 77–82 (2018).
46. Zhu, L. *et al.* Damage to dorsolateral prefrontal cortex affects tradeoffs between honesty and self-interest. *Nat. Neurosci.* **17**, 1319–1321 (2014).
47. Maréchal, M. A., Cohn, A., Ugazio, G. & Ruff, C. C. Increasing honesty in humans with noninvasive brain stimulation. *Proc. Natl. Acad. Sci.* **114**, 4360–4364 (2017).
48. Carter, R. M., Bowling, D. L., Reeck, C. & Huettel, S. A. A distinct role of the temporal-parietal junction in predicting socially guided decisions. *Science* **337**, 109–111 (2012).
49. Saxe, R. & Kanwisher, N. People thinking about thinking people. The role of the temporo-parietal junction in “theory of mind”. *NeuroImage* **19**, 1835–1842 (2003).
50. Samson, D., Apperly, I. A., Chiavarino, C. & Humphreys, G. W. Left temporoparietal junction is necessary for representing someone else’s belief. *Nat. Neurosci.* **7**, 499–500 (2004).
51. Schurz, M., Radua, J., Aichhorn, M., Richlan, F. & Perner, J. Fractionating theory of mind: A meta-analysis of functional brain imaging studies. *Neurosci. Biobehav. Rev.* **42**, 9–34 (2014).
52. Young, L., Cushman, F., Hauser, M. & Saxe, R. The neural basis of the interaction between theory of mind and moral judgment. *Proc. Natl. Acad. Sci.* **104**, 8235–8240 (2007).
53. Young, L., Camprodon, J. A., Hauser, M., Pascual-Leone, A. & Saxe, R. Disruption of the right temporoparietal junction with transcranial magnetic stimulation reduces the role of beliefs in moral judgments. *Proc. Natl. Acad. Sci.* **107**, 6753–6758 (2010).
54. Clithero, J. A. & Rangel, A. Informatic parcellation of the network involved in the computation of subjective value. *Soc. Cogn. Affect. Neurosci.* <https://doi.org/10.1093/scan/nst106> (2013).

55. Strombach, T. *et al.* Social discounting involves modulation of neural value signals by temporoparietal junction. *Proc. Natl. Acad. Sci. USA* **112**, 1619–1624 (2015).

Acknowledgements

We thank Liz Izakson for her help in data collection, and Dr. Xiaosi Gu for her thoughtful comments on the manuscript. This work was supported by National Science Foundation and US-Israeli Binational Science Foundation (NSF-BSF, Grant #0612015334) and the Israel Science Foundation (ISF, Grant #0612015023).

Author contributions

D.J.L. oversaw the project. A.S. and D.J.L. designed the experiment. A.S. collected and analysed the data. A.S. and D.J.L. wrote the manuscript.

Competing interests

The authors declare no competing interests.

Additional information

Supplementary information is available for this paper at <https://doi.org/10.1038/s41598-020-72255-5>.

Correspondence and requests for materials should be addressed to A.S.

Reprints and permissions information is available at www.nature.com/reprints.

Publisher's note Springer Nature remains neutral with regard to jurisdictional claims in published maps and institutional affiliations.



Open Access This article is licensed under a Creative Commons Attribution 4.0 International License, which permits use, sharing, adaptation, distribution and reproduction in any medium or format, as long as you give appropriate credit to the original author(s) and the source, provide a link to the Creative Commons licence, and indicate if changes were made. The images or other third party material in this article are included in the article's Creative Commons licence, unless indicated otherwise in a credit line to the material. If material is not included in the article's Creative Commons licence and your intended use is not permitted by statutory regulation or exceeds the permitted use, you will need to obtain permission directly from the copyright holder. To view a copy of this licence, visit <http://creativecommons.org/licenses/by/4.0/>.

© The Author(s) 2020